

Pyrrolysine Analogues

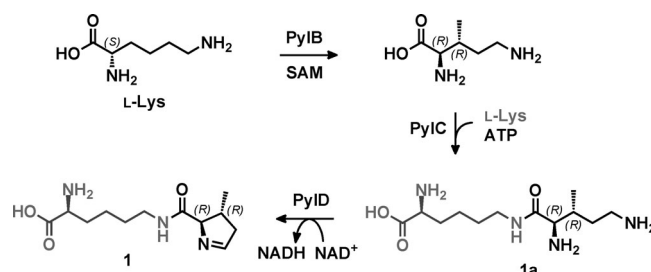
The Formation of Pyrroline and Tetrahydropyridine Rings in Amino Acids Catalyzed by Pyrrolysine Synthase (PylD)**

Felix Quitterer, Philipp Beck, Adelbert Bacher, and Michael Groll*

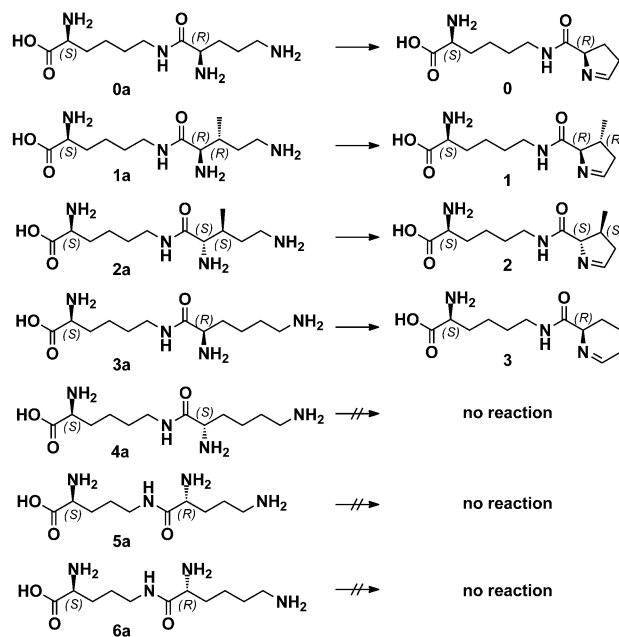
Abstract: The dehydrogenase PylD catalyzes the ultimate step of the pyrrolysine pathway by converting the isopeptide L-lysine-Nε-3R-methyl-D-ornithine to the 22nd proteinogenic amino acid. In this study, we demonstrate how PylD can be harnessed to oxidize various isopeptides to novel amino acids by combining chemical synthesis with enzyme kinetics and X-ray crystallography. The data enable a detailed description of the PylD reaction trajectory for the biosynthesis of pyrroline and tetrahydropyridine rings as constituents of pyrrolysine analogues.

Pyrrolysine (**1**) is the 22nd genetically encoded amino acid, which is incorporated into some proteins by means of ribosomal read-through of an amber stop codon (UAG) in certain methanogenic archaea and some eubacteria, including the human pathogen *Bilophila wadsworthia*.^[1] Pyrrolysine comprises a 4-methylpyrroline-5-carboxylate, which is linked by an isopeptide bond to Nε of L-lysine.^[1b] Recent studies revealed that the gene cluster *pylBCDST*^[2] orchestrates the biosynthesis of **1**^[3] (Scheme 1) and its insertion into the proteins MtmB, MtbB, and MttB,^[4] which function in the breakdown of methylamines.^[5]

Crystal structures of PylD in complex with the substrate and product surrogates L-lysine-Nε-D-ornithine (**0a**) and pyrroline-carboxy-lysine (**0**) revealed that the C-terminal lysine moiety is well coordinated, whereas the N-terminal unit only partially occupies the hydrophobic active site cavity, which is filled by a cluster of water molecules.^[3c] The aim of the presented work was to expand the scope of PylD substrates and harness the enzyme to oxidize isopeptides to novel amino acids (Scheme 2).



Scheme 1. Biosynthesis of pyrrolysine (**1**) starting from two L-lysine molecules. C-terminal and N-terminal parts of **1a** and **1** are depicted in gray and black, respectively. SAM = S-adenosylmethionine.



Scheme 2. Isopeptide substrates (**0a–6a**) and their respective products (**0–3**).

Since structural and functional data of PylD with its natural product pyrrolysine (**1**) have not been reported so far, we synthesized the substrate L-lysine-Nε-3R-methyl-D-ornithine (**1a**, Figure S1). Compound **1a** was cocrystallized with PylD and the complex structure was solved to 2.2 Å resolution (Figure 1a, for details see the Supporting Information). Inspection of the electron density map revealed that **1** has been formed. The structure displays that the L-lysine moiety of the isopeptide is enclosed in a hydrophobic channel, which is comprised by Leu3, Ile60, Phe63, and Ala103. The

[*] F. Quitterer,^[†] P. Beck,^[†] Prof. Dr. A. Bacher, Prof. Dr. M. Groll
Center for Integrated Protein Science Munich (CIPSM)
Lehrstuhl für Biochemie, Technische Universität München
Lichtenbergstrasse 4, 85748 Garching (Germany)
E-mail: michael.groll@tum.de

[†] These authors contributed equally to this work.

[**] We thank the staff of the beamline X06SA at the Paul Scherrer Institute, Swiss Light Source, Villigen (Switzerland) for their help with data collection and Katrin Gärtner for excellent technical assistance. Kinetic measurements were carried out by F.Q. at the Biological & Organometallic Catalysis (BOC) Laboratories of Prof. Dr. Jörg Eppinger, King Abdullah University of Science and Technology (KAUST), Thuwal, Saudi Arabia. This work was supported by the Hans-Fischer-Gesellschaft, by Award No. FIC/2010/07 from KAUST, and by the Deutsche Forschungsgemeinschaft (DFG, grant GR1861/7-1).

Supporting information for this article is available on the WWW under <http://dx.doi.org/10.1002/anie.201402595>.

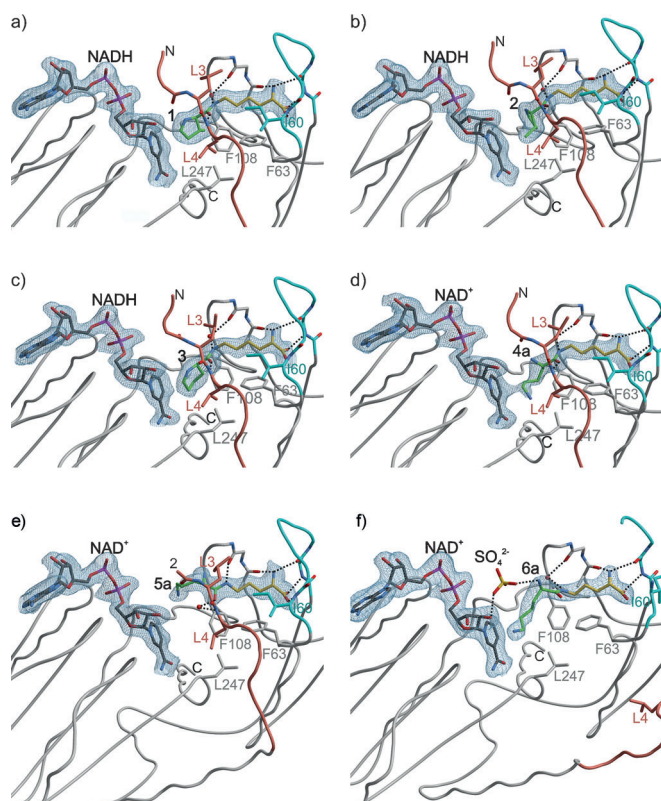


Figure 1. Active site of PylD in complex with a) **1**, b) **2**, c) **3**, d) **4a**, e) **5a**, and f) **6a**. The $2F_o - F_c$ electron density map is contoured at 1.0 σ . The N-terminus (amino acids 1–11) is shown in red and the loop connecting β -strand 1 and α -helix 3 (amino acids 55–59) is depicted in blue. The active-site residues and ligands are presented as stick models and water molecules are drawn as red spheres. Hydrogen bonds are indicated by dashed lines. Stereo views are presented in the Supporting Information (Figure S4).

carboxy and amino groups of the ligand are coordinated by direct and indirect hydrogen bonds to the backbone of PylD (for details see Figure S2a). The isopeptide motif is stabilized by an indirect hydrogen bond between its NH group and Asp104O via a defined water molecule, whereas the carbonyl oxygen interacts with Leu4NH of the N-terminal loop, participating in the induced-fit mechanism.^[3c] The N-terminal unit of **1** is oriented towards NADH with C5 of the pyrroline ring in proximity (4.0 Å) to C4 of the coenzyme's pyridine part. The 3*R*-methyl group of the pyrroline moiety displays van der Waals interactions with Phe63, Phe108, and Leu247, while the aliphatic ring is stabilized by the Leu4 side chain.

The structural data revealed that the closed active site cavity around the N-terminal part of **1** is spacious (ca. 450 Å³). Hence, we were interested in the stereospecificity of the enzyme and synthesized the diastereomer L-lysine-N ϵ -3*S*-methyl-L-ornithine (**2a**) and cocrystallized it with PylD. The $2F_o - F_c$ electron density map of the PylD:**2** complex (Figure 1b, 2.2 Å resolution) shows the conversion of **2a**, resulting in a tilted pyrroline ring in *S,S* configuration. Notably, the 3*S*-methyl group points towards the side chain of Leu4 and the nicotinamide ring of the coenzyme (for details see Figure S2b).

Inspired by the tolerated substrate spectrum of PylD, we designed further derivatives and synthesized L-lysine-N ϵ -D-lysine (**3a**) and L-lysine-N ϵ -L-lysine (**4a**) in which the N-terminal moiety of **0a** is extended by a CH₂ unit. The PylD:**3** complex structure (Figure 1c, 2.2 Å resolution) demonstrates that the D-lysine side chain is converted into a tetrahydropyridine ring (Figure S2c), whereas conversion of L-lysine-N ϵ -L-lysine (**4a**) is not catalyzed by PylD as shown by the complex structure (Figure 1d, 2.1 Å resolution) and by kinetic measurements (Table 1). The distance of the free ϵ' -amino group of

Table 1: Kinetic parameters for the conversion of PylD substrates. A detailed table, including K_m , k_{cat} , k_{cat}/K_m , and v_{max} for **0a** and **1a**, is provided in the Supporting Information (Table S2).

Substrate	Specific activity [nmol min ⁻¹ mg ⁻¹]	v_0 at 8 mM [nmol min ⁻¹]	Rel. activity at 8 mM [%]
0a	54.5 ^[3e]	10.2	72
1a	61.6	14.1	100
2a		3.4	24
3a		0.08	0.6
4a		< 0.001	< 0.01
5a		< 0.001	< 0.01
6a		< 0.001	< 0.01

4a to C4 of the coenzyme appears perfectly suitable for hydride transfer (3.3 Å, Figure S3a); however, an analysis of the rotational degrees of freedom of the terminal L-lysine side chain suggests that ring closure after preceding oxidation of the side chain would be hampered by steric interference with the walls of the active site cavity.

Since the C-terminal parts, including the isopeptide bonds, of the ligands **1a–4a** perfectly match each other by a root mean square deviation of less than 0.35 Å, we started to investigate its impact on enzyme catalysis. We placed L-ornithine as the C-terminal unit, resulting in L-ornithine-N δ -D-ornithine (**5a**) and L-ornithine-N δ -D-lysine (**6a**). Interestingly, the crystal structures of PylD:**5a** (Figure 1e, 2.2 Å resolution) and PylD:**6a** (Figure 1f, 2.2 Å resolution) depict both compounds at the active site, thus demonstrating that the driving force for binding strongly depends on the coordination of the carboxy and amino groups of the C-terminus. Since the C-terminal end of these analogues occupies the same position as in the previous examples, the isopeptide motif is forced to alter its location, orientation, and coordination as shown in Figure S3b,c. This is conducive to major alterations in the conformation of the amide substituents, which result in an unfavorable distance (6.3 Å) of the δ' -amino group from the pyridine nucleotide coenzyme to NAD⁺ in the case of **5a**, thus preventing catalysis.

So far, all described structures of PylD in complex with a ligand were obtained in the closed conformation. Hence, it was surprising that **6a** is fully defined in the electron density map, although the enzyme adopts its open state. Similar as in the PylD:holo structure,^[3c] the N-terminal residues (amino acids 1–11) do not cover the active site but extend the N-terminal helix. Furthermore, residues 55–59 of the loop coordinating the carboxy and amino groups of the C-terminal

moiety are structurally distorted. Though the terminal ϵ' -amino group is correctly orientated towards the coenzyme (4.3 Å to C4 of NAD⁺), **6a** was not transformed. These findings demonstrate that the closed state, which is not feasible in case of **6a** due to clashes with the PyID side chains of Leu3 and Leu4 (Figure S5), is crucial for catalysis. On the basis of the structural results, Leu4 seems to play a major role in the coordination and orientation of the N-terminal substrate moiety. In line with that, an L4A mutant did not show any detectable turnover of **1a** and therefore confirmed the major impact of this amino acid in the closed state.

A closer inspection of the PyID complex structures identified a set of organized water molecules in proximity to the N-terminal isopeptide part (Figure S6). Notably, this cluster is in contact with the heterocyclic nitrogen of all products through a defined solvent molecule at a distance of 2.6–3.1 Å (Figure 2a), which is absent in the electron density maps of the unreacted surrogates (Figure 2b). Due to the lack

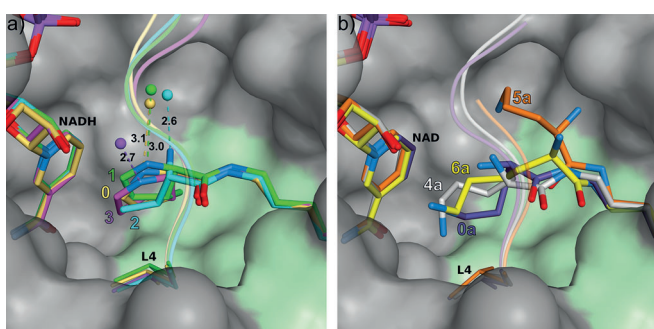
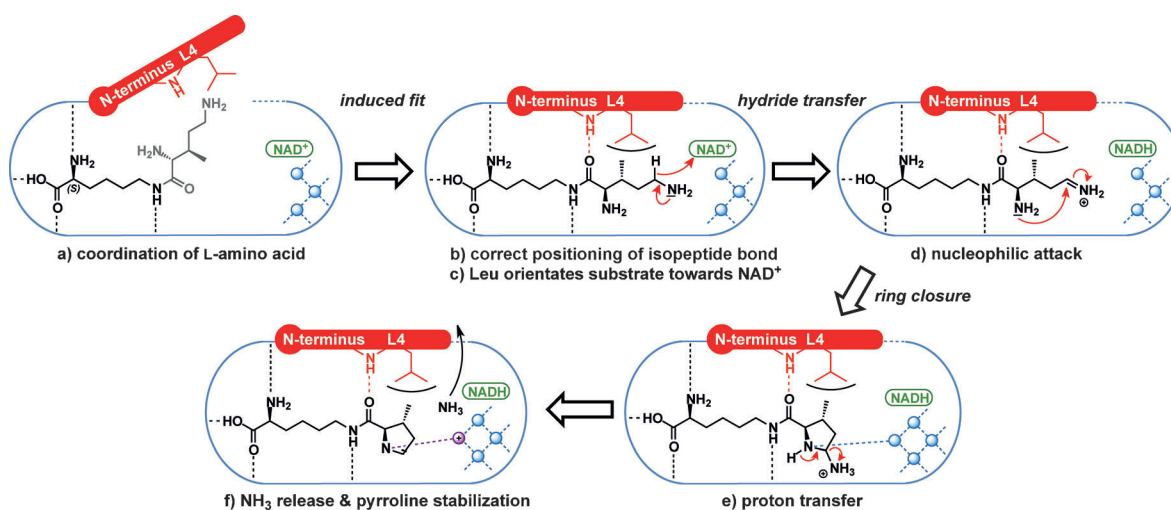


Figure 2. Superposition of PyID complex structures. The active site is shown for PyID:1 as a surface representation (gray). Hydrophobic amino acid side chains of PyID are colored in light green. The N-terminus of the protein is depicted as a transparent coil. a) Product structures **0–3**. Solvent molecules in contact with the heterocyclic nitrogen are shown as spheres; interactions are indicated by dashed lines (distances in Å). b) Substrate structures **0a** and **4a–6a**. Stereo views are presented in the Supporting Information (Figures S7 and S8, respectively).

of any activating amino acid in the active site, it appears reasonable that the terminal steps of PyID catalysis, in particular the addition of the α -amino group to the imine motif followed by the release of ammonia, are facilitated by the cluster. A related reaction, the conversion of L-ornithine to Δ^1 -pyrroline-5-carboxylate, is catalyzed by the enzyme ornithine δ -aminotransferase in plants. In contrast to the PyID substrates, ornithine is oxidized by transamination with 2-oxoglutarate.^[6]

The presented data on PyID complexes with substrate analogues in their open and closed conformations provide detailed insights into the reaction mechanism of PyID (Scheme 3):

- Ligand binding occurs in the open conformation, mainly driven by interactions of the C-terminal substrate part with the protein.
- The correct positioning of the ligand's isopeptide bond initiates the enzymatic induced fit, including amino acids 1–11 and 55–59.
- The substrate sensor Leu4NH forms a defined H-bond with the isopeptidic carbonyl oxygen of the ligand, resulting in an appropriate orientation of the N-terminal substrate moiety within the active site cavity.
- In addition, the Leu4 side chain restricts the active site cavity and forces the terminal amino group of the substrate towards NAD⁺ to enable hydride transfer. The resulting Schiff base is poised for a nucleophilic attack by the ligand's α amino group, resulting in a 2-aminopyrrolidinium intermediate.
- The closed active site encompasses a fixed network of water molecules that act as the proton shuttle, thus enabling proton release from the positively charged amino nitrogen. In particular, a single small molecule, H₂O or NH₃, interacting with the pyrroline or pyrrolidine nitrogen, was identified only in the product structures. This solvent molecule is in contact with the water cluster and therefore might initiate a proton transfer cascade, triggering the formation and release of **1**.



Scheme 3. Schematic representation of crucial substrate interactions and the reaction trajectory of PyID catalysis. Blue spheres represent fixed water molecules in proximity to the N-terminal substrate or product part. The purple sphere symbolizes a protonated water molecule.

The turnover rates and substrate affinities for **1a** reveal that PylD only possesses moderate activity ($K_m = 1.6 \text{ mM} \pm 0.18 \text{ mM}$, $k_{\text{cat}} = 1.72 \text{ s}^{-1} \pm 0.07 \text{ s}^{-1}$, Table S1). These findings are in good agreement with the proposed mechanism, since the enzyme lacks activating residues in the active site as well as elaborate specificity for the coordination of the N-terminal isopeptide moiety. Furthermore, PylD is subject to major conformational rearrangements, which so far is a singular case in the large family of dehydrogenases.

Nowadays, unnatural amino acids are indispensable in protein engineering as well as high-throughput technologies.^[7] We could show that primary amines with different stereochemical properties are well tolerated in the active site cavity of PylD. Thus, in vivo incorporation of pyrrolysine analogues into defined target proteins is also possible by utilizing the PylDST machinery, hereby obviating cost- and time-intensive chemical synthesis.

Received: February 19, 2014

Published online: June 10, 2014

Keywords: amino acids · dehydrogenases · enzyme catalysis · protein crystallography · pyrrolysine

- [1] a) G. Srinivasan, C. M. James, J. A. Krzycki, *Science* **2002**, *296*, 1459–1462; b) B. Hao, W. Gong, T. K. Ferguson, C. M. James, J. A. Krzycki, M. K. Chan, *Science* **2002**, *296*, 1462–1466; c) S. K. Blight, R. C. Larue, A. Mahapatra, D. G. Longstaff, E. Chang, G. Zhao, P. T. Kang, K. B. Green-Church, M. K. Chan, J. A. Krzycki, *Nature* **2004**, *431*, 333–335; d) C. Hertweck, *Angew. Chem.* **2011**, *123*, 9712–9714; *Angew. Chem. Int. Ed.* **2011**, *50*, 9540–9541; e) M. A. Gaston, R. Jiang, J. A. Krzycki, *Curr. Opin. Microbiol.* **2011**, *14*, 342–349.
- [2] D. G. Longstaff, R. C. Larue, J. E. Faust, A. Mahapatra, L. Zhang, K. B. Green-Church, J. A. Krzycki, *Proc. Natl. Acad. Sci. USA* **2007**, *104*, 1021–1026.
- [3] a) M. A. Gaston, L. Zhang, K. B. Green-Church, J. A. Krzycki, *Nature* **2011**, *471*, 647–650; b) S. E. Cellitti, W. Ou, H. P. Chiu, J. Grunewald, D. H. Jones, X. Hao, Q. Fan, L. L. Quinn, K. Ng, A. T. Anfora, S. A. Lesley, T. Uno, A. Brock, B. H. Geierstanger, *Nat. Chem. Biol.* **2011**, *7*, 528–530; c) F. Quitterer, A. List, W. Eisenreich, A. Bacher, M. Groll, *Angew. Chem.* **2012**, *124*, 1367–1370; *Angew. Chem. Int. Ed.* **2012**, *51*, 1339–1342; d) F. Quitterer, A. List, P. Beck, A. Bacher, M. Groll, *J. Mol. Biol.* **2012**, *424*, 270–282; e) F. Quitterer, P. Beck, A. Bacher, M. Groll, *Angew. Chem.* **2013**, *125*, 7171–7175; *Angew. Chem. Int. Ed.* **2013**, *52*, 7033–7037; f) J. A. Krzycki, *Curr. Opin. Chem. Biol.* **2013**, *17*, 619–625.
- [4] J. A. Soares, L. Zhang, R. L. Pitsch, N. M. Kleinholz, R. B. Jones, J. J. Wolff, J. Amster, K. B. Green-Church, J. A. Krzycki, *J. Biol. Chem.* **2005**, *280*, 36962–36969.
- [5] a) S. A. Burke, J. A. Krzycki, *J. Biol. Chem.* **1997**, *272*, 16570–16577; b) D. J. Ferguson, N. Gorlatova, D. A. Grahame, J. A. Krzycki, *J. Biol. Chem.* **2000**, *275*, 29053–29060; c) D. J. Ferguson, J. A. Krzycki, *J. Bacteriol.* **1997**, *179*, 846–852.
- [6] J. Stránská, D. Kopečný, M. Tylichová, J. Snégaroff, M. Šebela, *Plant Signaling Behav.* **2008**, *3*, 929–935.
- [7] a) B. H. Geierstanger, W. Ou, S. Cellitti, T. Uno, T. Crossgrove, H. P. Chiu, J. Grunewald, X. Hao, International patent application WO/2010/048582, **2010**; b) S. Lepthien, L. Merkel, N. Budisa, *Angew. Chem.* **2010**, *122*, 5576–5581; *Angew. Chem. Int. Ed.* **2010**, *49*, 5446–5450; c) E. Kaya, M. Vrabel, C. Deiml, S. Prill, V. S. Fluxa, T. Carell, *Angew. Chem.* **2012**, *124*, 4542–4545; *Angew. Chem. Int. Ed.* **2012**, *51*, 4466–4469; d) C. H. Kim, M. Kang, H. J. Kim, A. Chatterjee, P. G. Schultz, *Angew. Chem.* **2012**, *124*, 7358–7361; *Angew. Chem. Int. Ed.* **2012**, *51*, 7246–7249.